Nuclear Instruments and Methods in Physics Research B 267 (2009) 2769–2773

Contents lists available at ScienceDirect

Nuclear Instruments and Methods in Physics Research B

journal homepage: www.elsevier.com/locate/nimb

Competition of terrace and step-edge sputtering under oblique-incidence ion impact on a stepped Pt(1 1 1) surface

Yudi Rosandi [a], Alex Redinger [b], Thomas Michely [b], Herbert M. Urbassek [a,*]

[a] Fachbereich Physik, Technische Universität, 67663 Kaiserslautern, Germany
[b] II. Physikalisches Institut, Universität zu Köln, 50937 Köln, Germany

ARTICLE INFO

Article history:
Available online 28 May 2009

PACS:
61.80.Jh
79.20.Rf
68.49.Sf

Keywords:
Sputtering
Molecular-dynamics simulation
Ion reflection

ABSTRACT

Using molecular-dynamics simulation, we study the sputtering of a Pt(1 1 1) surface under oblique and glancing incidence 5 keV Ar ions. For incidence angles larger than a critical angle ϑ_c, the projectile is reflected off the surface and the sputter yield is zero. We discuss the azimuth dependence of the critical angle ϑ_c with the help of the surface corrugation felt by the impinging ion. If a step exists on the surface, sputtering occurs also for glancing incidence $\vartheta > \vartheta_c$. We demonstrate that for realistic step densities, the total sputtering of a stepped surface may be sizable even at glancing incidence.

1. Introduction

Ion impact at glancing incidence is particularly sensitive to surface defects. If the perpendicular energy of the ion is only of the order of a few tens of eV, the ion will be reflected specularly from the surface without inducing defect formation or sputtering. If the ion scatters at a surface defect – such as an adsorbate or an adatom, or as in the present work, a surface step – a substantial amount of the ion energy may be transferred to the surface, inducing defect formation and sputtering. This mechanism has been investigated recently both by molecular-dynamics simulation and by experimental measurements based on scanning tunneling microscopy [1–7]. The phenomenon is of immediate interest to the field of the nanopatterning of thin films [8,9] with applications, e.g. as a template for the adsorption of large molecules [10], for the manipulation of magnetism [11] or for tuning the chemical reactivity of catalytically active surfaces [12].

If the ion beam is inclined further from the target surface and the perpendicular energy of the ion increases, not only defects but also the flat terrace itself will contribute to sputtering. In the present paper, we address the question how the contribution of the flat terrace to sputtering starts increasing, and finally dominating, for less glancing incidence angles. At the same time, we inquire how the contribution of step edges to sputtering evolves as a function of the ion incidence angle. These questions will be answered for the specific case of 5 keV Ar impact on the Pt(1 1 1) surface, since this system has been characterized particularly well in the past [7]. The use of molecular-dynamics simulations allows us to study the sputter process in atomistic detail and in particular to include surface defects, such as the step edge, in a realistic way.

2. Method

Our MD simulation procedure is briefly described in the following [1,2]. The simulation target is a Pt crystallite with a (1 1 1) surface. For simulations with a flat target terrace, it contains about 19,210 atoms, arranged in nine layers. Each layer extends 160 Å in the direction of the ion velocity and is 87 Å broad. For simulations with a stepped target surface, the crystallite contains 62,144 atoms, arranged in 17 layers plus one half-layer on top of it. The size of the layers is 264×87 Å^2, and the half-layer was cut at a position 107 Å from the edge of the crystal to form an ascending B-step. In all cases, the crystallite is initially at 0 K.

We employ a many-body interaction potential [13] to describe the Pt–Pt interatomic interaction, which has been splined at high energies to the ZBL [14] potential. The Ar–Pt interaction is modeled to be purely repulsive according to the ZBL potential. The potentials are cut-off at 5.1 Å. We simulated the processes occurring after ion impact for 10 ps. Sputtered atoms are identified as those atoms which have no further interaction with the target surface. The data presented are averages over 100 events per unit cell for

* Corresponding author.
E-mail address: urbassek@rhrk.uni-kl.de (H.M. Urbassek).
URL: http://www.physik.uni-kl.de/urbassek/ (H.M. Urbassek).

0168-583X/$ - see front matter © 2009 Elsevier B.V. All rights reserved.
doi:10.1016/j.nimb.2009.05.051

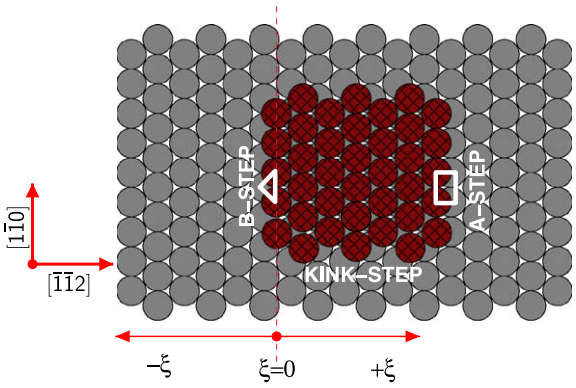

Fig. 1. Ball model of the (1 1 1) surface. The [$\bar{1}\,\bar{1}$ 2] and the [1 $\bar{1}$ 0] directions are shown by red arrows. The position of the ion impact point – measured at the height of the upper terrace – is denoted by ξ; $\xi = 0$ corresponds to the step-edge position. The ion impinges along the [$\bar{1}\,\bar{1}$ 2] azimuth in the vicinity of a B-step. (For interpretation of the references to colour in this figure legend, the reader is referred to the web version of this article.)

the flat-terrace simulations, and over 25 events for the stepped-surface simulations.

Fig. 1 shows a ball model of the (1 1 1) surface. The [$\bar{1}\,\bar{1}$ 2] and the [1 $\bar{1}$ 0] orientations as well as the three relevant kinds of steps on this surface are indicated. Here, we consider 5 keV Ar^+ impact on the flat terrace along the [$\bar{1}\,\bar{1}$ 2] and the [1 $\bar{1}$ 0] azimuth; additionally, we consider impacts along the [$\bar{1}\,\bar{1}$ 2] azimuth on the B-step. We denote the position of the ion impact points – measured at the height of the upper terrace – by ξ; $\xi = 0$ corresponds to the step-edge position.

3. Results

3.1. Ion reflection from a flat terrace

Fig. 2 shows the reflection coefficient of 5 keV Ar ions impinging with angle of incidence ϑ towards the surface normal onto a flat Pt(1 1 1) terrace. Each data point has been calculated by simulating 100 ion trajectories for 1 ps; each ion hits on another impact point on the unit cell of the Pt(1 1 1) surface. Here, we assume only those ions as reflected, which never penetrated into the target; i.e. $z > 0$ all the time. Fig. 2 demonstrates that for both azimuths studied, there exists a critical angle ϑ_c: For ion impacts with $\vartheta \geqslant \vartheta_c$, 100% of the projectiles are reflected off the surface. ϑ_c depends strongly on the impact azimuth; we have $\vartheta_c = 75^\circ$ for the [$\bar{1}\,\bar{1}$ 2] azimuth and $\vartheta_c = 82^\circ$ for the [1 $\bar{1}$ 0] azimuth.

In [7], we estimated the acceptance angles for (axial) channeling ψ_2 for 5 keV Ar ions in Pt using standard channeling theory [15]. We found $\psi_2 \cong 15^\circ$ for the [1 $\bar{1}$ 0] azimuth and $\psi_2 \cong 10^\circ$ for the [$\bar{1}\,\bar{1}$ 2] azimuth. Ion reflection at glancing incidence angles can be considered as *surface channeling*, since the ion is scattered almost elastically from the continuum potential of the first surface layer. For the [$\bar{1}\,\bar{1}$ 2] azimuth, ϑ_c roughly coincides with $90^\circ - \psi_2$; the deviations are due to the approximations of the surface potential entering into the simple estimate of ψ_2. The critical angle for the [1 $\bar{1}$ 0] azimuth is, however, considerably smaller than $90^\circ - \psi_2$. Here, in the angular range of around 68° and 82°, the reflection coefficient is reduced to around 0.7. For these angles, the ion remains axially channeled in the sense of bulk channeling theory, but it has a nonzero probability of jumping from the axial channel, into which it entered at the surface, to a deeper-lying channel and thus to be lost inside the target; in this case, the ion will not be reflected.

The quality with which the surface acts as a reflecting mirror can be assessed by discussing the surface corrugation. For the present case of interest, we quantify the corrugation with the help of

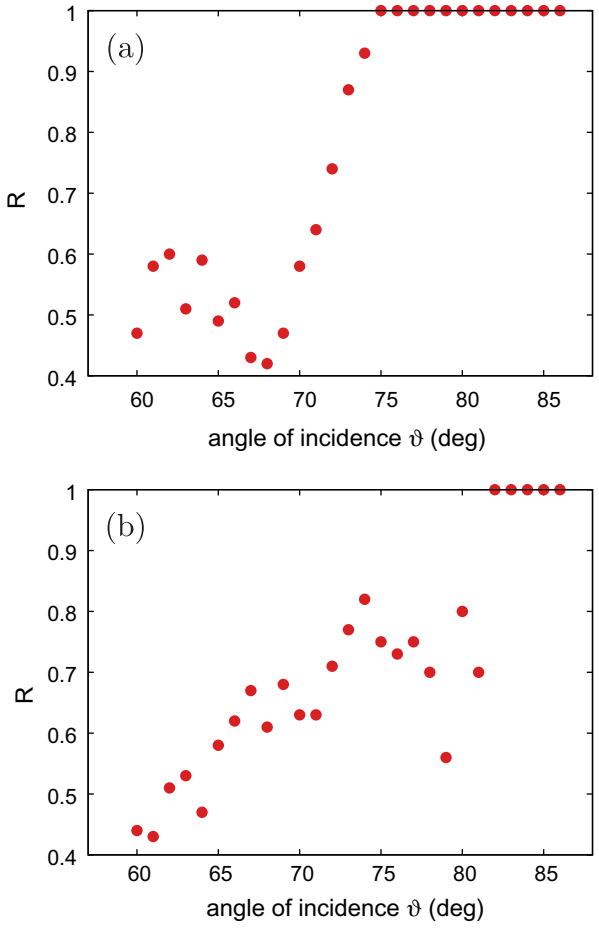

Fig. 2. Reflection coefficient R of a 5 keV Ar ion impinging on a Pt(1 1 1) surface as function of the angle of incidence. The projection of the ion impact direction to the surface is along the (a) [$\bar{1}\,\bar{1}$ 2] and (b) [1 $\bar{1}$ 0] azimuth.

the height $h(\boldsymbol{\rho})$ of the ion turning point in its motion above the reflecting surface. Here, $\boldsymbol{\rho} = (\ell, w)$ parameterizes the ion impact point on the surface unit cell, and $0 \leqslant \ell \leqslant L$ is the extension of the unit cell in axial direction (along the ion flight path), while $0 \leqslant w \leqslant W$ is the lateral dimension of the unit cell. Let us denote by $\Delta h(\ell)$ a measure of the lateral corrugation at axial position ℓ; we choose $\Delta h(\ell)$ as the difference between the highest and the lowest turning point height. Its average over ℓ then characterizes the lateral corrugation,

$$\langle \Delta h \rangle_{\text{lateral}} = \frac{1}{L} \int_0^L \Delta h(\ell) d\ell. \tag{1}$$

For the axial corrugation, we proceed analogously.

Fig. 3 shows the axial and lateral corrugations seen by the ion upon reflection off the surface for the [$\bar{1}\,\bar{1}$ 2] and [1 $\bar{1}$ 0] azimuth. A strong dependence on the azimuth is seen. When the ion approaches in the [1 $\bar{1}$ 0] direction, it sees the nearest-neighbor ⟨1 $\bar{1}$ 0⟩ atomic string in axial direction with virtually zero corrugation; in lateral direction, however, the surface is strongly modulated. For very glancing incidence, the perpendicular ion energy is small; the ion does not come close to the surface, and yet the corrugation amounts to 0.3 Å even for 86° incidence. For higher perpendicular energy, i.e. less glancing incidence, the ion feels the surface structure more closely and experiences an increased corrugation. We note that such a corrugation scenario is typical of axial channeling, here along the ⟨1 $\bar{1}$ 0⟩ atomic strings.

In contrast, for the [$\bar{1}\,\bar{1}$ 2] azimuth, the corrugations in axial and lateral direction are about similar. Note that even at 75° incidence

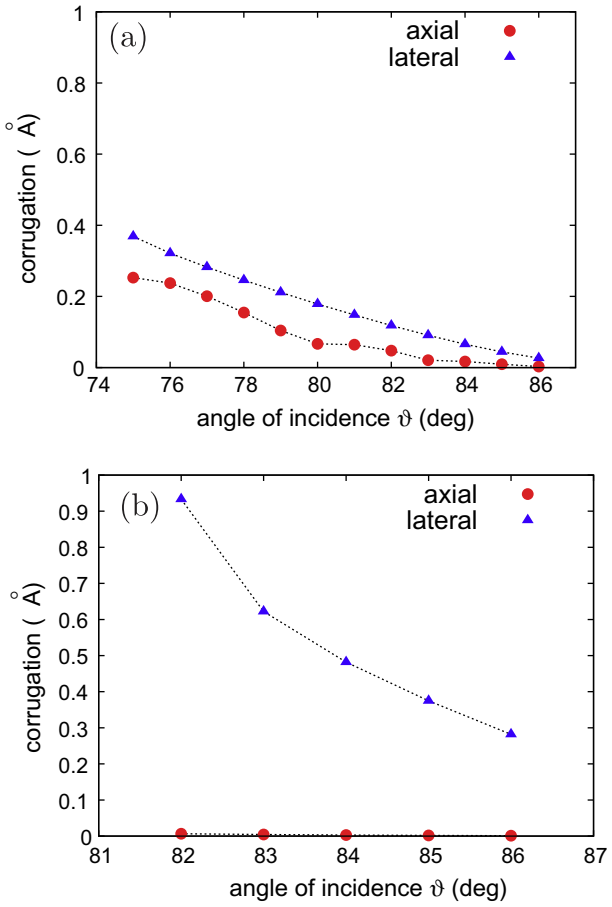

Fig. 3. Axial and lateral corrugation, cf. Eq. (1), of the Pt(1 1 1) surface as seen by a 5 keV Ar ion with incidence angle ϑ. The projection of the ion impact direction to the surface is along the (a) $[\bar{1}\,\bar{1}\,2]$ and (b) $[1\,\bar{1}\,0]$ azimuth.

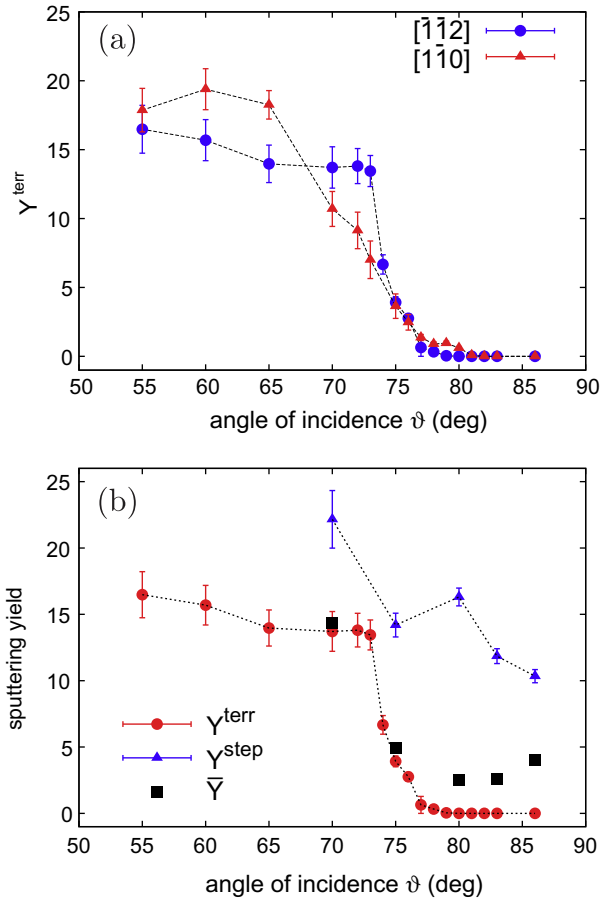

Fig. 4. (a) Comparison of terrace sputter yields as a function of incidence angle ϑ for the $[1\,\bar{1}\,0]$ and the $[\bar{1}\,\bar{1}\,2]$ azimuth. Error bars indicate the error in the average over 100 impact trajectories simulated per unit cell. (b) Molecular-dynamics data for the sputter yield of a flat terrace, Y^{terr} [7], and of a B-step, Y^{step}, as defined in Eq. (5), for 5 keV Ar impact on a Pt(1 1 1) surface at incidence angle ϑ. The projection of the ion impact direction to the surface is along the $[\bar{1}\,\bar{1}\,2]$ azimuth. The average sputter yield, $\bar{Y}$, has been calculated by Eq. (8) assuming a step density of $\rho_{\text{step}} = 6 \times 10^{-3}/\text{Å}$.

angle, the overall corrugation is quite moderate, when compared to the $[1\,\bar{1}\,0]$ azimuth. Such a situation is reminiscent of a planar channel.

Fig. 4(a) displays the sputtering data [7] induced by ion impact on a flat terrace for the two azimuths considered. For the $[\bar{1}\,\bar{1}\,2]$ azimuth, we observe a rather flat angular dependence between 55° and 73° incidence angle, followed by a sharp decrease. For $\vartheta > 80°$, the sputter yield is zero. This strong angle dependence is reminiscent of the channeling dips seen in bulk channeling experiments [16]. The coincidence of the angle at which the yield strongly decreases with the critical angle ϑ_c is satisfying. The behaviour for the $[1\,\bar{1}\,0]$ azimuth is similar for glancing incidence, $\vartheta \geqslant 75°$. However, the 'knee' present for the $[\bar{1}\,\bar{1}\,2]$ azimuth is missing here, and the sputter yield increase towards more oblique angles is more gentle. For angles around 55°, both azimuths give rise to the same sputter yields. We conclude that the planar channeling found for the $[\bar{1}\,\bar{1}\,2]$ azimuth gives rise to a clear channeling dip for sputtering, but not the axial channeling found for the $[1\,\bar{1}\,0]$ azimuth.

3.2. Sputtering from surface steps

The presence of a step on the surface changes the picture. For definiteness, we consider a B-step on the Pt(1 1 1) surface, with its step edge running in $[1\,\bar{1}\,0]$ direction. The ion impinges with $[\bar{1}\,\bar{1}\,2]$ azimuth from the lower terrace towards the ascending step edge. We measure distances perpendicular to the step edge by ξ, such that the step edge itself is located at $\xi = 0$. According to our geometrical model [1,7], ions which impinge in a region $-x_c \leqslant \xi \leqslant 0$ on the lower terrace may interact with the step edge. Here

$$x_c = 2\Delta h \cdot \tan\vartheta, \tag{2}$$

where $\Delta h = 2.26$ Å is the distance between the (1 1 1) layers.

We denote by $Y(\xi)$ the sputter yield induced by ions impinging at distance ξ from the step edge; in our simulations, $Y(\xi)$ is averaged over a surface unit cell. For glancing incidence, i.e. if the terrace does not contribute to sputtering, the step-edge sputter yield is given by

$$Y^{\text{step}} = \frac{1}{x_c}\int_{-\infty}^{\infty} Y(\xi)d\xi. \tag{3}$$

This notation clarifies that $Y^{\text{step}} \cdot x_c$ is actually the sputter cross-section of a step, normalized to unit step length. When the terrace also contributes to sputtering, as in our situation for less glancing incidence angles, it is convenient to define an excess yield by

$$Y^{\text{exc}} = \frac{1}{x_c}\int_{-\infty}^{\infty} [Y(\xi) - Y^{\text{terr}}]d\xi, \tag{4}$$

which allows to determine the full step-edge yield as

$$Y^{\text{step}} = Y^{\text{terr}} + Y^{\text{exc}}. \tag{5}$$

We display in Fig. 4(b) the step-edge yields for incidence angles $\vartheta \geqslant 70°$. It is seen that due to the contribution of the terrace yield, the determination of the step-edge yield has a higher error bar at smaller incidence angles. This error ϵ is calculated from the errors ϵ_ξ of the space dependent sputter yield data of Fig. 5 via [17]

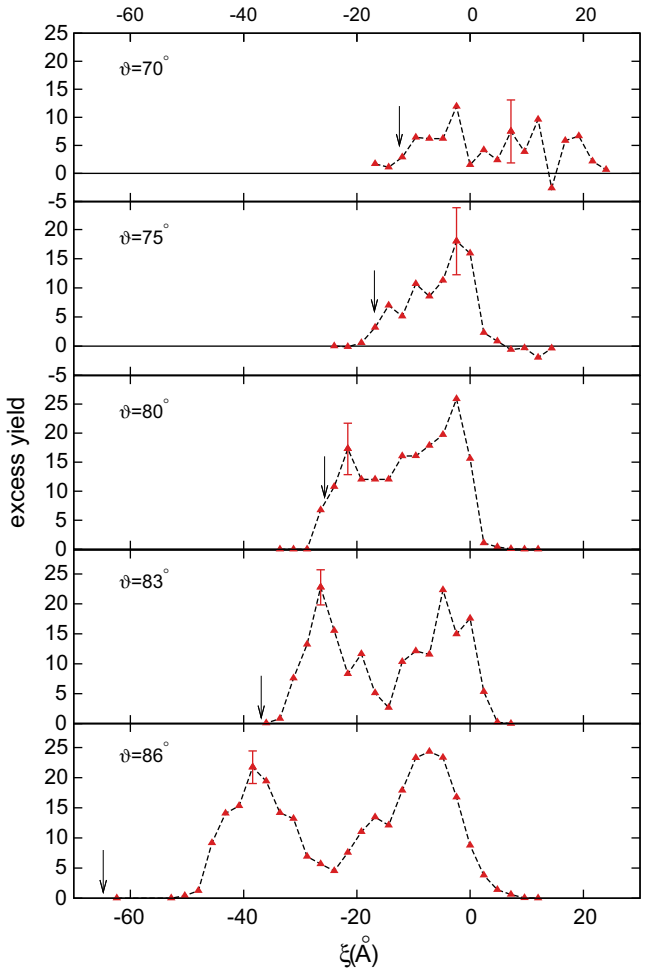

Fig. 5. Excess sputter yield, Eq. (4), of 5 keV Ar ions incident on a Pt(1 1 1) surface for various angles of incidence ϑ as a function of the distance ξ to a step located at $\xi = 0$. Negative ξ denote ion impact onto the lower terrace in front of the step. The projection of the ion impact direction to the surface is along the $[\bar{1}\,\bar{1}\,2]$ azimuth. The arrow indicates the position of $-x_c$, Eq. (2). The representative error bars indicate the error in the average over 25 impact trajectories simulated per unit cell.

$$\epsilon^2 = \sum_{\xi} \frac{(\epsilon_\xi)^2}{K^2}, \tag{6}$$

where K is the number of contributing ξ values. The step-edge yield is seen to have only a moderate angular dependence; its size is of similar magnitude as the terrace yield, $Y^{\text{terr}}(\vartheta < 73^\circ)$.

In a more general situation, steps will be present on a surface with a density ρ_{step}. The fractional surface area influenced by steps is given by

$$A^{\text{step}} = \rho_{\text{step}} \cdot x_c. \tag{7}$$

The average sputter yield of the surface is hence determined by the weighted average

$$\overline{Y} = A^{\text{step}} Y^{\text{step}} + (1 - A^{\text{step}}) Y^{\text{terr}}. \tag{8}$$

We include $\overline{Y}$ for a specific case in Fig. 4; $\rho_{\text{step}} = 6 \times 10^{-3}/\text{Å}$ has been chosen, as it is appropriate for a recent experiment [7]. Due to the strong angle dependence of x_c, the step-edge contribution becomes sizable at glancing incidence, even for widely spaced steps.

In Fig. 5, we display the ξ-dependence of the excess yield. For $\vartheta > 80^\circ$, $Y^{\text{step}} = Y^{\text{exc}}$, since $Y^{\text{terr}} = 0$. We note that for $\vartheta = 75^\circ$, $Y^{\text{terr}} = 3.9$ and for $\vartheta = 70^\circ$, $Y^{\text{terr}} = 14.2$. It is seen that for $\vartheta \geqslant 75^\circ$, indeed step (or excess) sputtering is limited to $-x_c \leqslant \xi \leqslant 0$, as predicted by the geometrical model. The case of 70° is special, since here the error bars are quite large, due to the interference with the terrace yields. It appears that in this case, also events with $\xi > 0$, i.e. ion impacts on the upper terrace contribute to enhanced sputtering, possibly, because the collision cascade induced now also encompasses step-edge atoms with their lower binding energy.

For $\vartheta = 83^\circ$ and 86°, $Y(\xi)$ has two major contributions, which have been termed the *direct-hit* ($\xi \cong 0$) and the *indirect-hit* ($\xi \cong -x_c$) contributions. The first contribution leads to sputtering, since these ions directly hit the exposed step-edge atoms and thereby impart energy to the target leading to sputtering. Ions of the former contribution are first reflected from the lower terrace and then hit the step-edge atoms also leading to sputtering. These two contributions are separated by a *channeling dip*; it could be shown that these ions are efficiently channeled between the two outermost surface layers of the upper terrace, contributing only little to sputtering [7].

Fig. 5 demonstrates that the channeling dip disappears already for $\vartheta = 80^\circ$. Furthermore, the simulations for $\vartheta = 80^\circ$ and 75° appear to indicate that the indirect-hit mechanism loses its importance; due to the steeper impact angle, reflected projectiles have a smaller chance to hit the step-edge atoms and to impart them sufficient energy for sputtering.

4. Conclusions

We study the incidence-angle dependence of sputtering at glancing incidence for the specific case of 5 keV Ar impact on the Pt(1 1 1) surface. We find:

1. A flat surface reflects ions completely for incidence angles larger than an (azimuth dependent) critical angle ϑ_c. Its azimuth dependence is discussed with the help of the surface corrugation felt by the impinging ion.
2. The sputter yield of a flat terrace quickly vanishes when ϑ reaches ϑ_c.
3. The presence of a surface step leads to sizable sputtering also for $\vartheta > \vartheta_c$.
4. Using realistic values for the step density on a vicinal Pt surface, we demonstrate that the effect of surface steps on sputtering at glancing incidence may be sizable.

Acknowledgement

The authors acknowledge support by the Deutsche Forschungsgemeinschaft.

References

[1] A. Friedrich, H.M. Urbassek, Surf. Sci. 547 (2003) 315.
[2] H. Hansen, C. Polop, T. Michely, A. Friedrich, H.M. Urbassek, Phys. Rev. Lett. 92 (2004) 246106.
[3] Y. Rosandi, H.M. Urbassek, Surf. Sci. 600 (2006) 1260.
[4] H. Hansen, A. Redinger, S. Messlinger, G. Stoian, Y. Rosandi, H.M. Urbassek, U. Linke, T. Michely, Phys. Rev. B 73 (2006) 235414.
[5] A. Redinger, H. Hansen, U. Linke, Y. Rosandi, H.M. Urbassek, T. Michely, Phys. Rev. Lett. 96 (2006) 106103.
[6] Y. Rosandi, H.M. Urbassek, Nucl. Instr. and Meth. B 256 (2007) 373.
[7] A. Redinger, Y. Rosandi, H.M. Urbassek, T. Michely, Phys. Rev. B 77 (2008) 195436.
[8] B. Ziberi, F. Frost, T. Höche, B. Rauschenbach, Vacuum 81 (2006) 155.
[9] W.L. Chan, E. Chason, J. Appl. Phys. 101 (2007) 121301.
[10] P. Chaudhari, J. Lacey, J. Doyle, E. Galligan, S.-C.A. Lien, A. Callegari, G. Hougham, N.D. Lang, P.S. Andry, R. John, et al., Nature 411 (2001) 56.
[11] R. Moroni, D. Sekiba, F. Buatier de Mongeot, G. Gonella, C. Boragno, L. Mattera, U.Valbusa, Phys. Rev. Lett. 91 (2003) 167207.
[12] L. Vattuone, U. Burghaus, L. Savio, M. Rocca, G. Costantini, F. Buatier de Mongeot, C. Boragno, S. Rusponi, U. Valbusa, J. Chem. Phys. 115 (2001) 3346.

[13] H. Gades, H.M. Urbassek, Nucl. Instr. and Meth. B 88 (1994) 218.
[14] J.F. Ziegler, J.P. Biersack, U. Littmark, The Stopping and Range of Ions in Solids, Pergamon, New York, 1985.
[15] J. Lindhard, Mat. Fys. Medd. K. Dan. Vidensk. Selsk. 34 (1965) 14.
[16] D.V. Morgan, Channeling: Theory, Observation and Applications, John Wiley, 1973.
[17] J.M. Hammersley, D.C. Handscomb, Monte Carlo Methods, Chapman and Hall, London, 1979.